Maximal Quantum Chaos of the Critical Fermi Surface

Maria Tikhanovskaya,[1] Subir Sachdev,[1,2] and Aavishkar A. Patel[3]
[1]*Department of Physics, Harvard University, Cambridge, Massachusetts 02138, USA*
[2]*School of Natural Sciences, Institute for Advanced Study, Princeton, New Jersey 08540, USA*
[3]*Department of Physics, University of California Berkeley, Berkeley, California 94720, USA*

(Received 14 February 2022; accepted 14 July 2022; published 3 August 2022)

We investigate the many-body quantum chaos of non-Fermi liquid states with Fermi surfaces in two spatial dimensions by computing their out-of-time-order correlation functions. Using a recently proposed large N theory for the critical Fermi surface, and the ladder identity of Gu and Kitaev, we show that the chaos Lyapunov exponent takes the maximal value of $2\pi k_B T/\hbar$, where T is the absolute temperature. We also examine a phenomenological model that can be continuously tuned between a non-Fermi liquid without quasiparticles and a Fermi liquid with quasiparticles. We find that the Lyapunov exponent becomes smaller than the maximal value precisely when quasiparticles are restored.

DOI: 10.1103/PhysRevLett.129.060601

The study of relaxational and thermalization phenomena in quantum many-body systems has long relied on the quasiparticle decomposition of many-body states, and the collisions of quasiparticles described by the Boltzmann equation and its generalizations. However, this powerful method is not reliable when we address similar phenomena in non-Fermi liquids without any quasiparticle excitations. General arguments have been presented that such dissipative phenomena cannot occur at a rate which is parametrically larger than $k_B T/\hbar$ as the absolute temperature $T \to 0$ (so such a rate cannot vanish as T^a, with an exponent $a < 1$), and systems without quasiparticles have a rate of order $k_B T/\hbar$ [1–6].

New insights into such issues have emerged from recent advances in the study of many-body quantum chaos and out-of-time-order correlators (OTOCs), for which the bounds on dissipative rates can be made precise. Inspired by holographic connections to the quantum dynamics of black holes, Maldacena, Shenker, and Stanford [7] established that the Lyapunov exponent, λ_L, characterizing the temporal growth of the OTOC must be smaller than $2\pi k_B T/\hbar$. We can expect that any system which is close to this bound as $T \to 0$ cannot have a quasiparticle description, and this conclusion is supported by computations on the Sachdev-Ye-Kitaev (SYK) model [8,9]. Although difficult to measure in experiments, OTOCs have therefore emerged as an alternative to the Boltzmann equation, and are a valuable diagnostic of the physics of nonquasiparticle systems.

In this Letter, we address the OTOC of a class of non-Fermi liquids most relevant to correlated electron systems [10]. We consider a Fermi surface coupled to a U(1) gauge field in two spatial dimensions, but our theory also applies to Fermi surfaces coupled to other critical bosons, as are realized near symmetry-breaking quantum phase transitions in metals with a zero momentum order parameter. The OTOC of such a system was addressed in previous work [11] in an uncontrolled analysis: it was found that $\lambda_L = \alpha k_B T/\hbar$ as $T \to 0$ with the constant $\alpha < 2\pi$. The present Letter will present new results on this model which build on two recent developments: (i) Gu and Kitaev (GK) [12] have shed new light on the structure of OTOCs in spatially extended systems. They established a ladder identity which shows that there is an additional contribution to the OTOC that arises from a pole at imaginary momentum, in the complex momentum plane. Provided the chaos butterfly velocity v_B is large enough, the pole contribution dominates at large spatial distances, and the resulting growth of the OTOC with time has exponent λ_L exactly equal to $2\pi k_B T/\hbar$. (ii) A systematic approach to the study of the two-dimensional non-Fermi liquid state has been proposed [13,14]. This approach obtains the non-Fermi liquid as the large N saddle point of a path integral over bilocal Green's functions and self energies. The new idea here is to study an ensemble of theories with different random couplings (but without spatial randomness), under the hypothesis that all of them flow to the same universal fixed point theory at low energies. Such a large N saddle point is ideally suited to develop a systematic computation of the OTOC, along the lines of computations on the SYK model.

In our large N analysis of the two-dimensional non-Fermi liquid, we find that the butterfly velocity does indeed satisfy the needed inequality of GK. This leads to our main result: that the Lyapunov exponent of this system equals the maximal value of $2\pi T$ ($\hbar = k_B = 1$ henceforth).

The model.—Our results are obtained within the "patch" theory of the two-dimensional non-Fermi liquid [15,16], which describes the low energy properties of the Fermi surface without quasiparticles. Each point on the Fermi

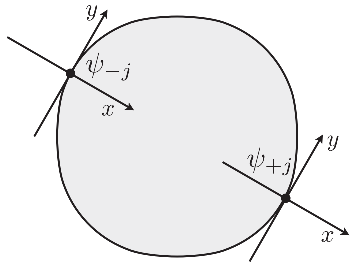

FIG. 1. Antipodal patches $\pm$ on the Fermi surface.

surface is characterized by a Fermi velocity v_F, and Fermi surface curvature κ/v_F. We introduce fermion fields $\psi_{\pm,j}$ ($j = 1 \ldots N$) defined in patches ($\pm$) near antipodal points, using the coordinate system shown in Fig. 1. The dispersion of the fermions in this coordinate system is $\varepsilon_{\boldsymbol{k}} = \pm v_F k_x + (\kappa/2) k_y^2$, and we will henceforth use length scales in which $v_F = 1$ and $\kappa = 2$. These fermions are coupled to bosons ϕ_l ($l = 1 \ldots M$), which is the transverse component of the gauge field, or a symmetry breaking order parameter. The universal properties of the critical Fermi surface in this patch theory are then described by the Lagrangian density

$$\mathcal{L} = \sum_{r=\pm} \sum_{j=1}^{N} \psi_{r,j}^\dagger (\partial_\tau - ir\partial_x - \partial_y^2) \psi_{r,j} + \sum_{r=\pm} \sum_{l=1}^{M} \sum_{ij=1}^{N} \frac{g_{ijl}}{N} r^s \psi_{r,i}^\dagger \psi_{r,j} \phi_l + \frac{1}{2} \sum_{i=1}^{M} (\partial_y \phi_i)^2. \tag{1}$$

Here $s = 0$ for the nematic order parameter, and $s = 1$ for the gauge field; the value of s will not be important for any results here. The large N limit [13] is taken at fixed M/N, and for an ensemble of theories with spatially uniform (but flavor random) Yukawa couplings g_{ijl}, which have zero mean and root mean square value g ($\overline{|g_{ijl}|^2} = g^2$). The scaling limit of the boson [$D(k)$] and fermion [$G_r(k)$] Green's functions can be computed exactly in the large N limit [$k = (\mathbf{k}, k_0) = (k_x, k_y, k_0)$, where k_0 is an imaginary Matsubara frequency]

$$D(k) = \frac{|k_y|}{|k_y|^3 + c_b |k_0| + m^2},$$
$$[G_r(k)]^{-1} = r k_x + k_y^2 - i\mu(T)\mathrm{sgn}(k_0) - i c_f \mathrm{sgn}(k_0) T^{2/3} H_{1/3}\left(\frac{|k_0| - \pi T \mathrm{sgn}(k_0)}{2\pi T}\right), \tag{2}$$

where $H_{1/3}(z) = \zeta(1/3) - \zeta(1/3, z+1)$ the analytically continued harmonic number function of order $1/3$, and c_f and c_b are coupling dependent constants:

$$c_f = \frac{M}{N} \frac{2^{4/3} g^{4/3}}{3^{3/2}}, \qquad c_b = \frac{g^2}{4\pi}. \tag{3}$$

We have also introduced a finite but small mass m^2 in the boson Green's function as an infrared regulator, and $\mu(T) = g^2 T/(3\sqrt{3} m^{2/3})$. We will eventually take the $m \to 0$ limit, and obtain a finite answer for the OTOC. To solve for the OTOC we use retarded and Wightman Green's functions, the forms of which we discuss in the Supplemental Material [17]. For simplicity, we will also henceforth consider only the $+$ patch on the Fermi surface and drop the patch indices [18]: in the Supplemental Material [17], we show that the interactions between antipodal patches do not change the behavior of the OTOC.

The OTOC.—We will be interested in the OTOC contained within the squared anticommutator of fermionic operators

$$\mathcal{C}_{\boldsymbol{x}}(t, 0) = \frac{1}{N^2} \theta(t) \sum_{i,j=1}^{N} \mathrm{Tr}[e^{-\beta H/2} \{\psi_i(\boldsymbol{x}, t), \psi_j^\dagger(0)\} \times e^{-\beta H/2} \{\psi_i(\boldsymbol{x}, t), \psi_j^\dagger(0)\}^\dagger]. \tag{4}$$

The function in (4) contains the OTOC $\langle \psi_i(\boldsymbol{x}, t) \psi_j^\dagger(0) \psi_i^\dagger(\boldsymbol{x}, t) \psi_j(0) \rangle$ (up to insertions of $e^{-\beta H/2}$), which describes chaos in the system and grows exponentially as $\sim e^{\lambda_L t} + \cdots$. We are interested in the spatial structure of (4) in the long time limit at large $|\boldsymbol{x}|$. After Fourier transforming the spatial arguments to momentum space, and considering 4 distinct times for the fermion operators (see Fig. 1 in the Supplemental Material [17]), we generalize the construction of Kitaev and Suh [9] to argue that the early time OTOC can be written using a single mode ansatz

$$\mathrm{OTOC}_{\boldsymbol{p}}(t_1, t_2, t_3, t_4; \boldsymbol{k}, \boldsymbol{k}') \approx \frac{e^{\lambda_L(\boldsymbol{p})(t_1+t_2-t_3-t_4)/2}}{C(\boldsymbol{p})} \Upsilon_{\boldsymbol{p}}^R(t_{12}, \boldsymbol{k}) \Upsilon_p^A(t_{34}, \boldsymbol{k}'). \tag{5}$$

Here the Υ's are vertex functions which only modify the overall magnitude of the OTOC. It was later shown by GK that the behavior of $C(\boldsymbol{p})$ is important for determining λ_L. As we review in the Supplemental Material [17], $C(\boldsymbol{p})$ has the important factor

$$C(\boldsymbol{p}) \sim \cos \frac{\lambda_L(\boldsymbol{p})}{4T}, \tag{6}$$

which vanishes at the maximal value of $\lambda_L(\boldsymbol{p}) = 2\pi T$. The resulting pole in (5) will ultimately be responsible for the maximal chaos in the non-Fermi liquid.

Now we can transform back to position space and obtain

$$\mathrm{OTOC}_{\boldsymbol{x}}(t_1,t_2,t_3,t_4) \sim \frac{u(\boldsymbol{x},t)}{N}\int_{\boldsymbol{k},\boldsymbol{k}'} \Upsilon^R_{\boldsymbol{p}}(t_{12},\boldsymbol{k})\Upsilon^A_{p}(t_{34},\boldsymbol{k}'), \quad (7)$$

where $t = (t_1 + t_2 - t_3 - t_4)/2$ and

$$u(\boldsymbol{x},t) \sim \int_{\boldsymbol{p}} \frac{e^{\lambda_L(\boldsymbol{p})t + i\boldsymbol{p}\cdot\boldsymbol{x}}}{\cos[\lambda_L(\boldsymbol{p})/(4T)]}. \quad (8)$$

In the previous work [11], the chaos exponent was identified with $\lambda_L(0)$. GK performed a careful evaluation of the integral in (8) in one spatial dimension, and gave conditions under which it was dominated by the saddle point $[\lambda_L'(p = p_s)t + ix = 0]$ or the pole $[\lambda_L(p = p_1) = 2\pi T]$. Both the saddle point and the pole appear for purely imaginary values of momenta, with $p = i|p|$. When $|p_s| > |p_1|$, GK showed that the pole dominates, leading to a region of spacetime in which maximal chaos occurs. Conversely, when $|p_s| < |p_1|$, the saddle point dominates, and there is no maximal chaos.

At first sight, it is not clear whether this one-dimensional analysis can be extended to the anisotropic two-dimensional non-Fermi liquid theory in (1). However, the theory in (1) has a "sliding symmetry" [16], which implies that λ_L is a function only of $p_x + p_y^2$. This reduces the momentum integral in (8) to effectively a one-dimensional integral, and we can replace $\boldsymbol{p}\cdot\boldsymbol{r}$ by $p_x x$ and directly apply the results of GK.

The Lyapunov exponent.—The remaining missing ingredient in determining whether the saddle point or the pole dominates for the critical Fermi surface is a knowledge of $\lambda_L(p)$ for imaginary p. For this we need to solve the Bethe-Salpeter equation for the squared anticommutator $\mathcal{C}$ in Fig. 2, with an imaginary external momentum. This leads to the following eigenvalue equation, extending the previously obtained equation [11] to an imaginary external momentum $p_x = i|p_x|$

$$\begin{aligned}
&\left\{c_f T^{2/3}\left[H_{1/3}\left(\frac{-ik_0 - \pi T}{2\pi T}\right) + H_{1/3}\left(\frac{-i(\omega - k_0) - \pi T}{2\pi T}\right)\right] - |p_x| + 2\mu(T)\right\}\mathcal{C}(k_0,\omega,i|p_x|)\\
&\quad = g^2\frac{M}{N}\int\frac{dk_0' dk_y'}{(2\pi)^2}\frac{c_b(k_0 - k_0')|k_y'|}{(|k_y'|^3 + m^2)^2 + c_b^2(k_0 - k_0')^2}\frac{\mathcal{C}(k_0',\omega,i|p_x|)}{\sinh\frac{k_0 - k_0'}{2T}}\\
&\qquad + \frac{g^{4/3}4\pi^{4/3}}{3\sqrt{3}}\frac{M}{N}\int\frac{dk_0' dk_{01}}{(2\pi)^2}\frac{(ik_{01} + (-ik_{01})^{2/3}(i(k_{01} - \omega)))}{k_{01}(i(k_{01} - \omega))^{1/3}(2k_{01} - \omega)}\frac{\mathcal{C}(k_0',\omega,i|p_x|)}{\cosh\frac{k_0 - k_{01}}{2T}\cosh\frac{k_0' - k_{01}}{2T}}. \quad (9)
\end{aligned}$$

We note that the factors of M/N on the rhs of (9) cancel with those in the definition of c_f in the $m \to 0$ limit, up to a rescaling of $p_x \to (N/M)p_x$. Therefore, considering $M \neq N$ will not affect any of our conclusions, and we will henceforth consider $M = N$ for simplicity.

Maximal chaos.—Upon solving the eigenvalue equation (9), we obtain the Lyapunov exponent as a function of the external imaginary momentum $p_x = i|p_x|$. From Fig. 3, the values of the pole ($p_1 = i|p_1|$) and saddle point ($p_s = i|p_s|$) momenta can be obtained. The pole follows from $\lambda_L(p = p_1) = 2\pi T$, whereas for the saddle point, one needs to consider an additional condition, since the saddle

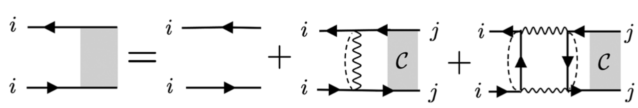

FIG. 2. The Bethe-Salpeter equation for $\mathcal{C}(k_0,\omega,i|p_x|)$, which is exact at large N. Solid lines are fermion propagators, wavy lines are boson propagators, and dashed lines are averaging over the flavor random couplings. The horizontal lines represent the retarded Green's functions and vertical lines are Wightman propagators.

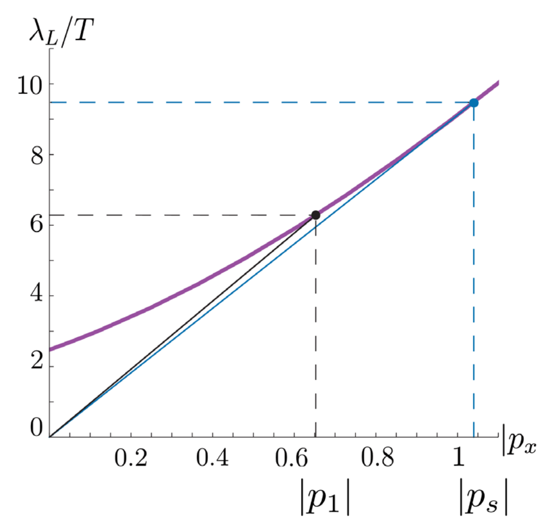

FIG. 3. Plot of the Lyapunov exponent λ_L/T as a function of $|p_x|$. $|p_x|$ is presented in units of $g^{4/3}T^{2/3}$. We find $|p_1| \approx 0.65 g^{4/3}T^{2/3}$ and $|p_s| \approx 1.04 g^{4/3}T^{2/3}$. Since $|p_s| > |p_1|$, the butterfly velocity is given by $v_B = 2\pi T/|p_1| \approx 9.67 g^{-4/3}T^{1/3}$ (slope of the black solid line). We also find the value of the velocity at the saddle point $v_s = 9.01 g^{-4/3}T^{1/3}$ (slope of the blue solid line). As expected from previous work [11], we find $\lambda_L(0) = 2.48T$.

point equation $\lambda_L'(p = p_s)t + ix = 0$ does not define the value of $|p_s|$. This condition follows from the fact that the ansatz (7) is valid only in the regime where initial correlations and nonlinear effects can be ignored, which is when $\mathrm{OTOC}_{\boldsymbol{x}}(t_1, t_2, t_3, t_4) \gg 1/N$, and therefore $u(\boldsymbol{x}, t) \sim 1$. This gives the condition on the saddle point value $\lambda_L(p = p_s)t + ip_s x = 0$ [12]. Combining this equation with the saddle point equation, we can then obtain $|p_s|$ from the graphical solution of $\lambda_L'(p = p_s) = \lambda_L(p = p_s)/|p_s|$.

As shown in Fig. 3, $|p_1|$ is significantly smaller than $|p_s|$. Specifically, we find $|p_1| \approx 0.65 g^{4/3} T^{2/3}$ and $|p_s| \approx 1.04 g^{4/3} T^{2/3} > |p_1|$, which confirms the dominance of the pole contribution according to GK. The chaos wavefront therefore travels with a butterfly velocity $v_B = 2\pi T/|p_1|$ set by the pole contribution. We note that $\lambda_L(p_x)$ does not depend upon the coupling g, as g can be removed by rescaling the external momentum $p_x \to p_x/g^{4/3}$. With no other dimensionful parameters in (9), this also implies that λ_L is proportional to temperature.

Phenomenological models.—We extend our analysis to non-Fermi liquids with dynamical critical exponent $2 < z \leq 3$, in which quasiparticle excitations are still absent, and compute the Lyapunov exponents. For those theories, the boson Green's function has the form [13]

$$D(k) = \frac{|k_y|}{|k_y|^z + c_b|k_0| + m^2},$$

and the fermion self energy scales as $\Sigma \sim i\,\mathrm{sgn}(k_0)|k_0|^{2/z}$ ($z = 3$ for the original theory discussed earlier). Since $|\Sigma| \gg |k_0|$, quasiparticle excitations are not well defined in terms of the fermion spectral function.

The form of the eigenvalue equation for the OTOC changes slightly, and is discussed in the Supplemental Material [17]. As we show in the Fig. 4, for each of these theories the butterfly velocity is also given by $v_B = 2\pi T/|p_1|$, and the Lyapunov exponent is maximal. To show this, we first solve the eigenvalue equations up to the pole momentum p_1. We then compare the instantaneous slope at p_1, which we call v_*, and the velocity $v_1 = 2\pi T/|p_1|$. For each plot we obtain $v_1 > v_*$. Since each of the curves in Fig. 4 is a positive, monotonically increasing, and convex function, this implies that $|p_s| > |p_1|$, and the pole contribution therefore dominates with maximal chaos just like in the $z = 3$ case. We can further find the behavior of the exponent in the Fermi liquid case of $1 < z < 2$, in which quasiparticles are present. In this regime, $|\Sigma| \sim |k_0|^{2/z} \ll |k_0|$, and therefore the quasiparticle peak in the fermion spectral function is well defined. Similar to the discussion above, we can compute the Lyapunov exponent as a function of external momentum on imaginary axis and explicitly find $|p_s|$ and $|p_1|$. For a particular case of $z = 3/2$ [19], we find that the saddle point dominates as $|p_s| \approx 4.32$, which is smaller than $|p_1| \approx 7.84$. The resulting butterfly velocity in this case

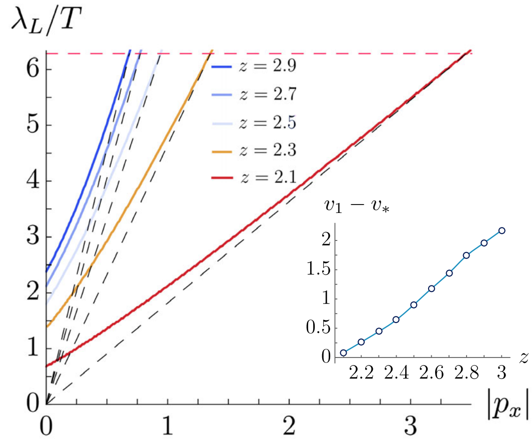

FIG. 4. Main plot: resulting plots of the Lyapunov exponent λ_L/T as a function of $|p_x|$, for different values of the dynamical critical exponent $2 < z \leq 3$. The slopes of the black dashed lines are the butterfly velocities v_B. Inset: difference between $v_1 = v_B$ and the instantaneous slopes at $p_x = p_1$ (i.e., v_*). The difference is always positive, i.e., $\lambda_L(i|p_1|)/|p_1| > \lambda_L'(i|p_1|)$, which shows that the value of $|p_s|$, where $\lambda_L(i|p_s|)/|p_s| = \lambda_L'(i|p_s|)$, must be larger than $|p_1|$, leading to maximal chaos according to GK.

is $v_B \approx 0.8 v_F$, where $v_F = 1$ is the Fermi velocity. This result is expected from a general point of view: for a free fermion theory the exponent is a simply linear function of the external momentum $\lambda_L(i|p_x|) = |p_x|$ leading to the saddle point contribution at $|p_s| = 0$. We therefore expect that for any theory with quasiparticles, the pole contribution is negligible compared to a saddle point contribution, and the maximal chaos is no longer present (Supplemental Material [17]).

Discussion.—It is quite remarkable that the generic low energy theory of Fermi surfaces without quasiparticles in two spatial dimensions displays maximal chaos in the large N limit. Other spatially extended models connected to the SYK model (e.g., [20,21]), and certain conformal field theories [22–24], have been shown to display maximal chaos, but none of them have spatially dependent Green's functions *and* live in more than one spatial dimension. It is also remarkable that the critical Fermi surface displays maximal chaos without the presence of conformal symmetry, which also sets it apart from the previously mentioned examples that have conformal symmetry.

We believe that the maximal chaos of the Fermi surface is linked to the local nature of the singular self energy of the fermion at large N, i.e., the self energy is frequency dependent, but independent of momentum, a feature the Fermi surface theory shares with the SYK model (along with the local frequency-only dependence of the fermion pairing vertex [13]). There are small contributions to the fermion anomalous dimension at 3-loop order [16], which are expected to make the self energy nonlocal, and it remains to be seen if such effects could reduce the maximal Lyapunov exponent. However, since $|p_s| - |p_1|$ is $\mathcal{O}(1)$

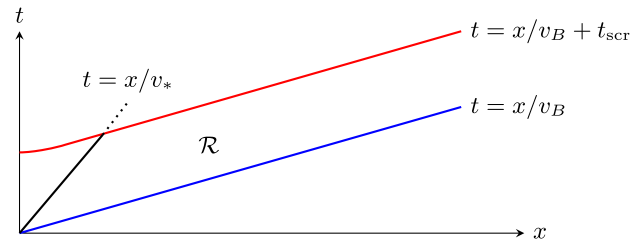

FIG. 5. (Adapted from GK) Maximal chaos is present in the spacetime region denoted by $\mathcal{R}$, which is bounded by the three solid lines. Here $v_* = \lambda_L'(i|p_1|)$, and $t_{\rm scr} \sim \ln N$. As z is reduced from 3 to 2, v_* approaches $v_B = v_1$ from below (Fig. 4), and the size of the maximally chaotic region $\mathcal{R}$ is therefore squeezed to zero by the falling slope of the black line as $z \to 2$. For $z < 2$, there is consequently no maximally chaotic region.

at large N (Fig. 3), we expect that the small $\mathcal{O}(1/N)$ corrections to this quantity will not immediately be able to change its sign and thus reduce the maximal Lyapunov exponent.

We also examined a phenomenological model of a critical Fermi surface with dynamic critical exponent $z \le 3$; quasiparticles reemerge in such a model for $z < 2$. We found that the maximal chaos was retained for precisely the regime where quasiparticles are absent, $2 < z \le 3$, although the size of the spacetime region for which it occurs shrinks to zero as $z \to 2$ (Fig. 5). It is also remarkable that the acceleration of chaos to the maximal rate by the butterfly effect is tied to the destruction of quasiparticles in this model. When quasiparticles are present, we found that the saddle-point contribution dominated with $\lambda_L \sim T^{2/z} \ll T$, which is parametrically smaller than the maximal rate (Supplemental Material [17]).

We thank Haoyu Guo and Yingfei Gu for valuable discussions. M. T. and S. S. were supported by the National Science Foundation under Grant No. DMR-2002850. A. A. P. was supported by the Miller Institute for Basic Research in Science. This work was also supported by the Simons Collaboration on Ultra-Quantum Matter, which is a grant from the Simons Foundation (651440, S. S.).

[1] S. A. Hartnoll and A. P. Mackenzie, Planckian dissipation in metals, arXiv:2107.07802.
[2] D. Chowdhury, A. Georges, O. Parcollet, and S. Sachdev, Sachdev-Ye-Kitaev models and beyond: A window into non-Fermi liquids, arXiv:2109.05037.
[3] S. Sachdev, *Quantum Phase Transitions* (Cambridge University Press, Cambridge, UK, 1999), 10.1017/CBO9780511973765.
[4] J. A. N. Bruin, H. Sakai, R. S. Perry, and A. P. Mackenzie, Similarity of scattering rates in metals showing T-linear resistivity, Science **339**, 804 (2013).
[5] J. Zaanen, Why the temperature is high, Nature (London) **430**, 512 (2004).
[6] G. Grissonnanche, Y. Fang, A. Legros, S. Verret, F. Laliberté, C. Collignon, J. Zhou, D. Graf, P. A. Goddard, L. Taillefer, and B. J. Ramshaw, Linear-in temperature resistivity from an isotropic Planckian scattering rate, Nature (London) **595**, 667 (2021).
[7] J. Maldacena, S. H. Shenker, and D. Stanford, A bound on chaos, J. High Energy Phys. 08 (2016) 106.
[8] J. Maldacena and D. Stanford, Remarks on the Sachdev-Ye-Kitaev model, Phys. Rev. D **94**, 106002 (2016).
[9] A. Kitaev and S. J. Suh, The soft mode in the Sachdev-Ye-Kitaev model and its gravity dual, J. High Energy Phys. 05 (2018) 183.
[10] S.-S. Lee, Recent developments in non-Fermi liquid theory, Annu. Rev. Condens. Matter Phys. **9**, 227 (2018).
[11] A. A. Patel and S. Sachdev, Quantum chaos on a critical Fermi surface, Proc. Natl. Acad. Sci. U.S.A. **114**, 1844 (2017).
[12] Y. Gu and A. Kitaev, On the relation between the magnitude and exponent of OTOCs, J. High Energy Phys. 02 (2019) 075.
[13] I. Esterlis, H. Guo, A. A. Patel, and S. Sachdev, Large N theory of critical Fermi surfaces, Phys. Rev. B **103**, 235129 (2021).
[14] E. E. Aldape, T. Cookmeyer, A. A. Patel, and E. Altman, Solvable theory of a strange metal at the breakdown of a heavy Fermi liquid, Phys. Rev. B **105**, 235111 (2022).
[15] S.-S. Lee, Low-energy effective theory of Fermi surface coupled with U(1) gauge field in $2+1$ dimensions, Phys. Rev. B **80**, 165102 (2009).
[16] M. A. Metlitski and S. Sachdev, Quantum phase transitions of metals in two spatial dimensions. I. Ising-nematic order, Phys. Rev. B **82**, 075127 (2010).
[17] See Supplemental Material at http://link.aps.org/supplemental/10.1103/PhysRevLett.129.060601 for detailed derivations.
[18] For the theory with only one patch, the values of c_f, c_b are given by $c_f = (M/N)2^{5/3}g^{4/3}/3^{3/2}$ and $c_b = g^2/(8\pi)$.
[19] The numerical values of $|p_s|$ and $|p_1|$ are provided for chosen parameters $g = 0.5$, $\Lambda = 50$, $T = 1$, and $z = 3/2$. See Supplemental Material [17] for more details.
[20] Y. Gu, X.-L. Qi, and D. Stanford, Local criticality, diffusion and chaos in generalized Sachdev-Ye-Kitaev models, J. High Energy Phys. 05 (2017) 125.
[21] J. Kim, E. Altman, and X. Cao, Dirac fast scramblers, Phys. Rev. B **103**, L081113 (2021).
[22] G. J. Turiaci and H. Verlinde, On CFT and quantum chaos, J. High Energy Phys. 12 (2016) 110.
[23] F. M. Haehl and M. Rozali, Effective field theory for chaotic CFTs, J. High Energy Phys. 10 (2018) 118.
[24] F. M. Haehl, W. Reeves, and M. Rozali, Reparametrization modes, shadow operators, and quantum chaos in higher-dimensional CFTs, J. High Energy Phys. 11 (2019) 102.